

Laboratory and Numerical Investigation of Saltwater Intrusion into Aquifers

S. Noorabadi, A.A. Sadraddini*, A.H. Nazemi, R. Delirhasannia

Department of Water Engineering, University of Tabriz, Tabriz, Iran

*Received 12 Nov 2016,
Revised 01 Jan 2017,
Accepted 10 Jan 2017*

Keywords

- ✓ Concentration variation,
- ✓ Head fluctuation,
- ✓ Interface,
- ✓ Laboratory experiment,
- ✓ Saltwater recession,
- ✓ SEAWAT

alisadraddini@yahoo.com
Tel: (+984133392792)

Abstract

Laboratory methods along with numerical solutions are suitable methods to study the process of seawater intrusion (SI) into aquifers. In this study, we successfully visualized the saltwater intrusion process in a laboratory scale model. Also the SI process was numerically simulated using the SEAWAT model to validate the physical model results. The effects of saltwater concentration variations and freshwater head gradient changes on the interface movement and how they influence the interface behavior in recession and intrusion stages, were key points of this study. Results showed that the saltwater with C2 concentration (50g/L) intruded into a greater part of the aquifer than that with the concentration of C1 (35g/L). Moreover, intruding rates of the fresh-salt water interface by application of the C2 concentration were faster than those by application of the C1 one in all the experiments. In the both concentrations, raising the freshwater level by 0.5 cm caused the interface to recede about 30 cm and vice versa. Comparing the intruding and receding data under an identical experimental condition showed that the recession time of the fresh-salt water interface was less than its intrusion time, which was an important result in SI management. We also analyzed the dispersion effect and measured the mixing zone thickness as 2.5 cm. Finally the velocity vector analysis was done to investigate the saltwater and freshwater velocities under the steady state conditions. Furthermore, comparison of the SEAWAT simulation results with the experimental data showed a good agreement between them.

1. Introduction

Groundwater is generally the most important freshwater resource in many coastal regions which, are usually threatened by seawater intrusion (SI) [1]. Saltwater intrusion is a natural process where seawater would advance into the coastal groundwater aquifers due to the density different between saline and fresh waters, creating an evolving wedge toward the land [2]. The SI process is caused by prolonged changes (or in some cases severe episodic changes) in coastal groundwater levels due to pumping, land-use and climate changes or sea-level fluctuations [3]. This problem increasingly becomes more severe as the coastal population increases. With about 70% of the world's population living in coastal zones, the challenges are for the optimum exploitation of the fresh groundwater and the control of seawater intrusion [4]. Therefore, understanding the dynamics and behavior of saltwater intrusion into aquifers is an important research issue.

A wide variety of large-scale, laboratory-scale and numerical models for investigating the SI process have been provided in the literature. Understanding the saltwater movement in a field-scale aquifer is a complex task. Therefore, most of the experimentalists have studied (and visualized) the saltwater wedges in laboratory-scale physical models using different colored waters instead of field scale investigations [5]. Besides the mentioned advantage, due to the low cost, less time consuming and possibility of studying different scenarios under controlled conditions, the laboratory-scale models have been considered by many researchers in recent years. In these studies, a laboratory scale box with the certain dimensions containing a homogeneous sand medium with relatively high hydraulic conductivity has been used [2, 6-8].

Chang and Clement [6] studied experimentally and numerically the effects of two major climate change-induced hydrological variables, i.e. sea level rise and reduction of groundwater fluxes, on saltwater intrusion process. They also simulated the experimental conditions using the numerical code SEAWAT. They

hypothesized that when the fluxes are perturbed, it would take relatively less time for a saltwater wedge to recede from an aquifer, as compared to the time needed to advance into the aquifer. They applied a combination of the laboratory and numerical experiments to investigate this hypothesis and explained the reason for the difference in intrusion rates on the basis of the resulted data.

Zhang et al. [9] implemented experimental and numerical investigations to study the transport and fate of a contaminant plume along saltwater boundary in the vicinity of a steady state condition. Their goal was to identify the result of simplifying the seaward boundary condition by eliminating the seawater density and tidal fluctuations. They reported that eliminating the density effects led to underestimation of the solute discharge rates and incorrect prediction of the solute migration pathways.

Chang and Clement [6] completed both the laboratory and numerical experiments to investigate the contaminant transport in the vicinity of a saltwater wedge. They used SEAWAT to investigate the experimental data, saltwater flow and transport dynamics within a wedge. Their laboratory data showed that the transport rates acting above the wedge almost were twice faster than the transport rates acting within the wedge for the small-scale experimental system which was characterized by very low level of mixing. Their numerical results showed that for large-scale systems involving higher levels of mixing (or dispersion) the transport rate acting within the wedge could be comparable or even higher than the rates acting above the wedge.

Goswami and Clement [7] considered transport processes associated with advance and recession of the SI under varying hydraulic gradients using a sand box experiments. They also used SEAWAT model for simulation of the model condition. They concluded that the proposed benchmark was stronger and might be used as an alternative to the traditional Henry problem [10].

Morgan et al. [11] used a physical sand tank to model a sea level rise and seawater intrusion in a flux-controlled unconfined aquifer setting for consideration of the measurability of SI overshoot process. Their results showed that an overshoot can occur for the case of a retreating interface. The magnitude of the overshoot for sea level fluctuation in the physical experiments was 24% of the change in steady state interface position.

The objective of this study is to investigate saltwater intrusion dynamics through experimental and numerical methods. We have used a laboratory box to directly map the interface treatment and used SEAWAT model to numerically study the SI process. Two different saltwater concentrations have been used to study the effects of saltwater concentration variation on the SI process. The freshwater level is changed in order to study the interface intruding and receding treatments. At the end, a comprehensive study of saltwater wedge patterns using numerical results has been presented. This is first time that a comprehensive and simultaneous investigation of SI including saltwater concentration variation, head gradient, dispersion effect and saltwater interface dynamics through experimental and numerical methods is presented. Previous literature has focused on limited aspects of the SI process in their works.

2. Materials and methods

2.1. Experimental method

Figure 1 shows the experimental box used in this study. The box was constructed using steel plates at back, right and left sides and a Plexiglas plate at the front side. There were two chambers at the left and right sides of the box as the reservoirs of the saltwater and freshwater, respectively. Also a chamber was placed between the mentioned side chambers in the central part of the box that was filled with silica sand up to the height of 50 cm. The average diameter of the sand grains was 1 mm. The internal dimensions of the central chamber were 110cm×100cm×5cm (length*height*thickness) and both the side chambers had 5cm length and were separated from the porous sand medium chamber by two fine mesh sheets. This narrow tank was used to simulate the two-dimensional flow of an unconfined aquifer. The water heads in the side chambers were controlled by the two adjustable tanks that were connected to them. Saltwater was prepared by dissolving commercial salt in tap water in a large tank. Furthermore, a tap spot was set at the top of saltwater chamber to discharge the overflow coming from the freshwater chamber. The salinities of the fresh and salt water were measured using a laboratory bench-top meter. The concentration of saltwater for the first set of the experiments was determined 35 g/L (named

experiment 1) and for the second set it was 50 g/L (named experiment 2) and the concentration of the freshwater (tap water) was 0.25 g/L. Density of the saltwater were about 1.025 g/cm³ and 1.04 g/cm³. This saltwater was colored by a red food dye to distinguish it from the freshwater. Some researchers have used food dye in their laboratory scale experiments successfully (e.g. food color [12]; potassium permanganate/fluorescein [13]; Rhodamine WT [14, 15]; food dye [3, 4, 7], food color, New Coccine Acid Red 18 (C.I. Number 16255) [8]). In this study, about 5 g dye was added to 10 liters of saltwater. A digital camera (Canon PowerShot SX520 HS) was used to take pictures during the experiments. The hydraulic conductivity (K) of the replaced sand in the tank was measured using the in-situ method described in Simmons et al. [15] and Darcy law. The average value of the estimated conductivity was 1 cm/s. For determining the dispersivity coefficients, we used the methods mentioned in the literatures. Some researchers have used the average grain diameter as the longitudinal dispersivity value and assumed the transverse dispersivity value to be about 1/10 of the longitudinal dispersivity amount [7,8,16]. Some others have used the calibration method to determine these coefficients [5,6]. In the present study, the value of longitudinal dispersivity was firstly assumed to be 1 mm, equal to the average diameter of the grains with a transverse dispersivity values of 0.01 mm. We also determined these coefficients by calibrating the numerical results with the experiments. The results of these two methods had a good correspondence, so the assumed values of the dispersivity coefficients were accepted. The average porosity of the porous medium was measured by both the volumetric and gravitational methods and its value was 0.38. Table 1 shows all the experimental parameters used in this study.

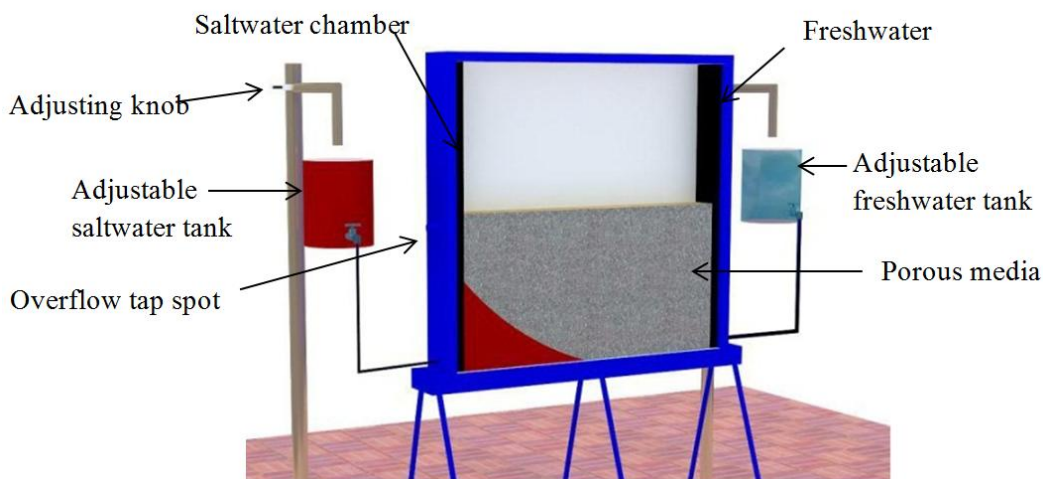


Figure 1: Details of the experimental box used in this study

Table 1: Experimental parameters

parameter	Value
Porous sand medium dimensions	50cm × 110cm × 5 cm
Hydraulic conductivity	1 cm/s
Porosity	0.38
Saltwater concentration	35, 50 g/L
Saltwater density	1.025, 1.04 g/cm ³
Freshwater concentration	0.25 g/L
Longitudinal dispersivity	0.001 m
Transverse dispersivity	0.0001 m

2.2. Experiments Implementation

The porous medium tank was packed under saturated conditions in layers of 5 cm to avoid air entrapment. The porous medium and chambers were initially filled with tap water from the overhead freshwater tank. First, a freshwater flow was applied from right to the left at constant gradient condition ($h_{salt} = 47 \text{ cm}$, $h_{fresh} =$

48 cm) so all the porous medium was filled by freshwater. The hydraulic conductivity of the porous medium was measured using the in situ method by applying different fixed gradient conditions and measuring the fluxes. After reaching the steady state condition, the saltwater intrusion process was initiated toward the left side chamber by opening the saltwater reservoir gate. The dense and dyed saltwater invaded the porous medium and this process was recorded by taking photos every 2 minutes. The system was allowed to reach the steady state condition. When there was no observable change in the location of the fresh-salt water interface, it could be concluded that the steady state condition had been obtained (named as test 1). Then, the head gradient was changed by adjusting the head of freshwater ($h_{salt} = 47 \text{ cm}$, $h_{fresh} = 48.5 \text{ cm}$). Consequently, the saltwater wedge started to move back to reach another steady state condition (named as test 2). When the second steady state condition was established, the third stage of the experiment started by returning the freshwater head back to the test 1 condition. This caused the saltwater wedge to invade forward and led to the same steady state condition of the test 1 (this stage named as test 3). These gradient changes were for studying and comparing the intrusion and recession treatments of saltwater wedge under the above mentioned stages and conditions. As mentioned before, these experiments were done under two different saltwater concentrations (C1= 35 g/L, C2 = 50 g/L). The saltwater injection rate into the left chamber was adjusted so that a fixed 45 cm head of saltwater in this reservoir was established. The upper 2 cm freeboard was assigned for flushing freshwater from the porous medium. This flushing water exited the box by overflowing through an adjustable tap.

2.3. Numerical simulation

We used the MODFLOW family variable density flow code SEAWAT [12] to model the experimental data. This model has been widely used to simulate SI process in laboratory scale studies [6,7,8]. In our modelling, a rectangular domain indicated the porous medium (with the same dimensions of the physical model). The lower left-hand corner of the domain was set as the origin of an x-z coordinate system. For applying the finite difference numerical approach, the domain was discretized in horizontal and vertical directions. The grid horizontal and vertical sizes were 2 and 1 cm, respectively. The right and left boundaries were set as constant head boundary conditions. Besides, the left boundary was assigned as a constant concentration boundary with the saltwater concentration amounts of 35 g/L and 50 g/L at the experiments C1 and C2, respectively. The right boundary at both of the experiments C1 and C2 had a constant concentration of 0.25 g/L. The lower and upper boundaries were considered as no-flow condition. Initially the entire domain of the flow was filled by the freshwater and under a constant head gradient there was a steady flow from the right boundary to the left boundary. Hence, the initial concentration at entire domain of the model was assigned to 0.25 g/L. The other required input parameters of the model were applied in accordance to the experimental condition. The SEAWAT model uses the coupled flow and solute transport equations as follow:

$$\frac{\partial}{\partial \alpha} \left(\rho K_{f\alpha} \left[\frac{\partial h_f}{\partial \alpha} + \frac{\rho - \rho_f}{\rho_f} \frac{\partial Z}{\partial \alpha} \right] \right) + \frac{\partial}{\partial \beta} \left(\rho K_{f\beta} \left[\frac{\partial h_f}{\partial \beta} + \frac{\rho - \rho_f}{\rho_f} \frac{\partial Z}{\partial \beta} \right] \right) + \frac{\partial}{\partial \gamma} \left(\rho K_{f\gamma} \left[\frac{\partial h_f}{\partial \gamma} + \frac{\rho - \rho_f}{\rho_f} \frac{\partial Z}{\partial \gamma} \right] \right) = \rho S_f \frac{\partial h_f}{\partial t} + \theta E \frac{\partial C}{\partial t} - \bar{\rho} q_s \quad (1)$$

$$\frac{\partial C}{\partial t} = \nabla \cdot (D \cdot \nabla C) - \nabla \cdot (vC) - \frac{q_s}{\theta} C_s \quad (2)$$

Equations 1 and 2 are flow and solute transport equations respectively. In these equations, α , β , γ are the components of principle axes, ρ [ML⁻³] is the fluid density, K [LT⁻¹] is the hydraulic conductivity of the porous media, h [L] is the water head, Z [L] is the elevation of the specified point, subscript of 'f' refers to freshwater, S_f [L⁻¹] is the specific storage in terms of freshwater head, θ [-] is the porosity, E [-] is the ratio between the fluid density and solute concentration, C [ML⁻³] is the solute concentration, $\bar{\rho}$ [ML⁻³] is the density of water entering from a source or leaving through a sink, q_s [T⁻¹] is the volumetric flow rate per unit volume of aquifer representing sources and sinks, v [LT⁻¹] is the fluid viscosity, D [L²T⁻¹] is the hydrodynamic dispersion coefficient and C_s [ML⁻³] is the solute concentration of water entering from sources and sinks. The SEAWAT

model uses the finite difference method to solve the flow equation. This model also uses the MT3DMS [17] code to solve the solute transport equation.

3. Results and discussion

3.1. Experimental observations

Investigation of the behavior and dynamics of fresh-salt water interface was done on the basis of the 3 conducted tests of SI process. These 3 tests were implemented under two different saltwater concentrations (i.e. $C_1=35$ g/L and $C_2=50$ g/L). The first test (or test 1) included the saltwater intrusion from the beginning up to reach the steady state condition. The test 2 started by increasing the freshwater level to 48.5 cm and included the recession process of the saltwater wedge until it reached another steady state condition. Test 3 started by decreasing the freshwater level back to its initial level of 48 cm to allow the fresh-salt water interface to be reached the first steady state condition (end of test 1).

Figure 2 shows the process of saltwater intrusion in the experiment C1 at the test 1 (named as C1T1). The first row shows the depicted experimental results and second row shows the simulation results of SEAWAT. We used photos taken at 10, 20 and 70 min after beginning of the test 1 to show the SI process. The heads of salt and fresh waters at the left and right boundaries were fixed at the levels of 47 and 48 cm respectively. This caused the freshwater to transmit from the right chamber to the left chamber. A density driven flow caused the saltwater interface to be moved under the freshwater. As it is shown in the figures, the saltwater invades towards the freshwater which finally leads to the establishment of steady flow. Since the head gradient in the vicinity of saltwater chamber was high in early times, then the rate of the wedge invasion was fast and decreased over the time and finally the system reached the steady state condition in about 60 minutes. The location of two critical points (i.e. the saltwater toe at the bottom (X_{toe}) and the saltwater wedge elevation at the left inlet (Z_w) could be determined by analyzing the photos. The location of the wedge toe (X_{toe}) at the first steady state condition had a distance of 60 cm from the coordinate origin (at $Z=0$) and the elevation of the wedge at saltwater inlet (Z_w) was 40 cm (at $X=0$).

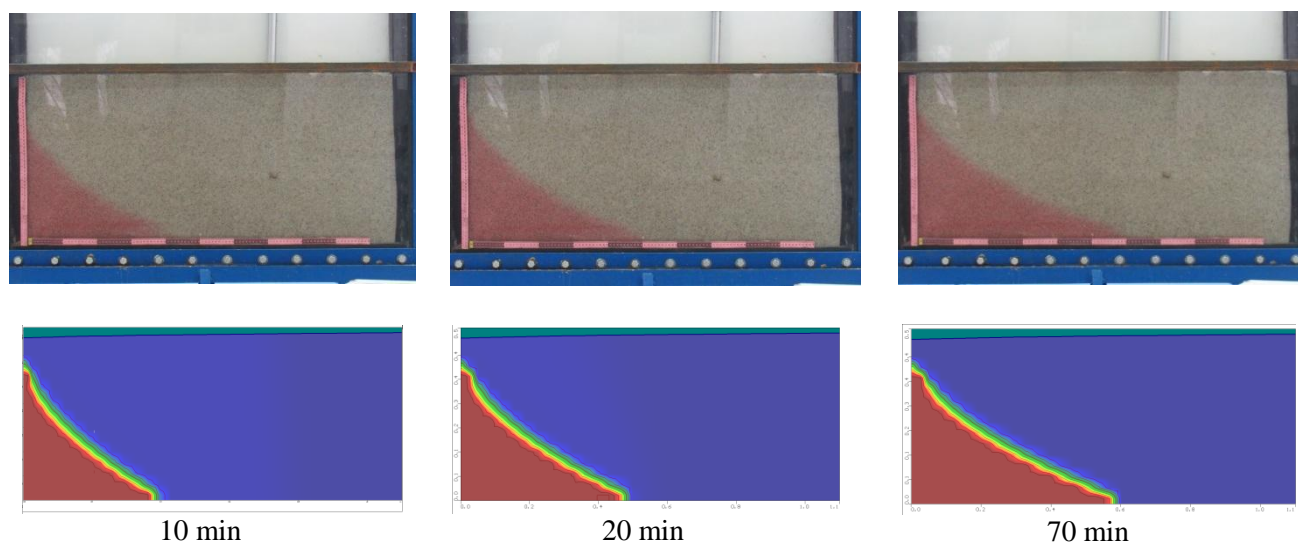


Figure 2: Intrusion process of the saltwater in concentration of the C1 at the test 1. Experimental and modeling results.

After establishing a steady state condition, the freshwater head was increased up to 48.5 cm to allow more freshwater to be flown from the right to the left which caused backward movement of the saltwater wedge (recession stage). Figure 3 shows the backward movement of the wedge in the times of 10, 20 and 35 minutes after the beginning of the second stage. The recession stage ended and the system reached the second steady state condition in 35 minutes. The locations of the critical points under the second steady state condition were fixed at the coordinates of $X_{toe}= 27$ cm and $Z_w= 26$ cm.

As mentioned before, by returning the freshwater head to its initial condition (i.e. 48 cm) at the third stage, again the intrusion of saltwater was started and provided a suitable condition for comparison of the saltwater recession and advance times and also their rates in the same scale. A detailed comparison and analysis of the recession and invasion stages are presented in the following parts.

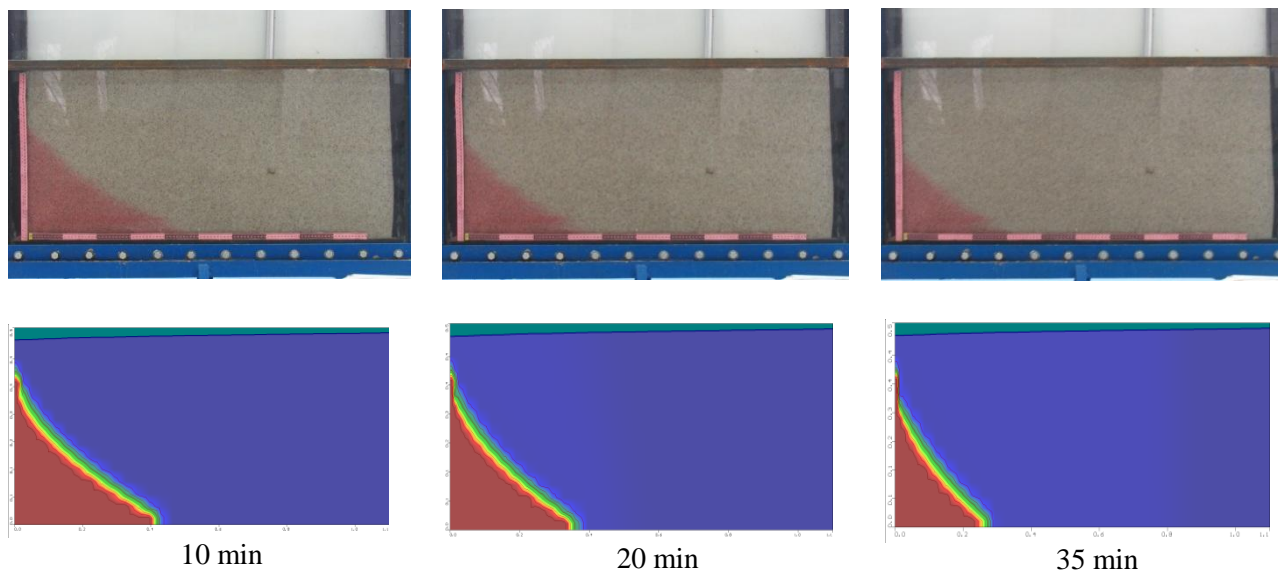


Figure 3: Recession process of the saltwater interface in the concentration of C1 after increasing the freshwater head (test 2)

The experiments were repeated for a different salt concentration ($C=50$ g/L). Figure 4 shows the related results. As shown in these photos, advancing rate of saltwater interface is faster than that in previous experiment ($C1=35$ g/L).

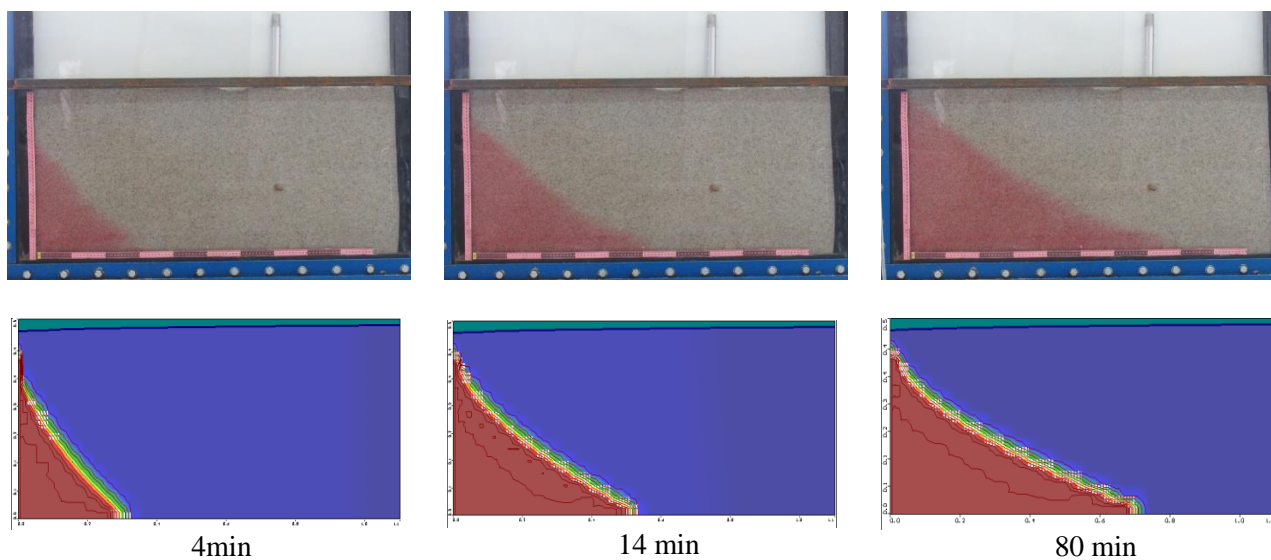


Figure 4: Intruding process of the saltwater interface in the experiment C2

Furthermore, when the system reached a steady state condition (see column 3 in figure 4), the location of the toe had a further distance from the origin of the coordinates and also the elevation of the wedge at the inlet was higher, in comparison to those in the experiment C1. The experiment C2 reached the steady state condition after 70 minutes. The photos of figure 4 show the intrusion process of the wedge at 4, 14 and 80 minutes after the start of the experiment C2. In this experiment, the locations of the two critical points under the steady state condition were fixed at the coordinates of $X_{toe}=75$ cm and $Z_w=43$ cm. The tests 2 and 3 were repeated for the experiment C2 under the same hydraulic condition explained already for the experiment C1. The photos of the

recession stage for C2 are not illustrated here because of their extra volume. Also the analysis of these processes is mentioned in the following.

3.2. Modeling results

In this study, we used the finite difference model of SEAWAT [12] to simulate the experiments. Our goal was to validate the experimental data and to investigate whether the experimental data were consistent with the predictions made by the model. Figures 2, 3 and 4 show the graphical results of the model compared with the experimental photos. As shown in the pictures, the model has predicted the SI process in all scenarios successfully. Figure 2 (C1T1) shows that the model accuracy improves by the time passed. When the system reached the steady state condition, the prediction accuracy of the model reached its maximum amount. Because the left column grid served as the saltwater boundary condition grid, so the model prediction at the inlet wedge shaped a little swelling. Figure 3 shows the results of the experiment C1T2. Figure 4 relates the results of the experiment C2, indicating a good accuracy of the model in prediction of the experiment condition which even is better than that in the experiment C1.

For accurate investigation of the experimental and numerical results, comparison of the data has been done and the result is shown in the charts of figure 5. In this figure, dot-shaped symbols represent the experimental data and the continuous lines represent the SEAWAT prediction of 50% concentration contour. As shown in the figure, there is a reasonable match between the model and experimental results. However, SEAWAT predictions show less accuracy in early times. Generally, the predicted wedge levels near the inlet are almost a little bit higher than experimental amounts, also the predicted distances of the wedge toe are smaller than the experimental values, hence for visual considerations, these differences are presented in fig. 5. Goswami and Clement [7] have related these minor incompatibilities to some difficulties in maintaining a constant freshwater head level during the initial phase. In our study, the minor variations of the overflow level at saltwater chamber in early unsteady stages could be a similar reason for these incompatibilities. In addition, the experiment C2 has a better match with the predicted data than the experiment C1.

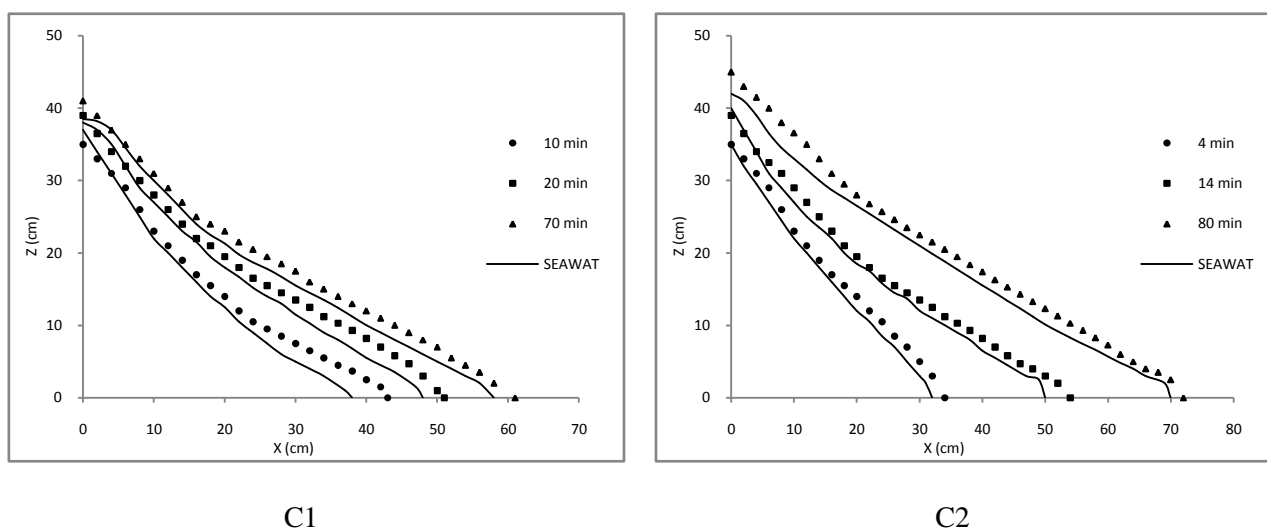


Figure 5: Comparison of the saltwater wedge movement between the experimental data and SEAWAT results

3.3. Dispersion effect

The mixing zone of freshwater and seawater in a coastal aquifer controls regional groundwater flow dynamics and reactive transport processes [5]. There are three basic processes operating to transport solutes: diffusion, mechanical dispersion and advection. Diffusion is the process by which the molecules dissolved in water move from areas of higher concentration to areas of lower concentration. Advection is the process by which moving ground water carries with it dissolved solutes. Mechanical dispersion is the process whereby solutes are mechanically mixed during advective transport, caused by the velocity variations at the microscopic level. Due

to mechanical dispersion and molecular diffusion, which drive salt into the outflowing freshwater thereby contributing to the convective circulation within the wedge, the salt concentration and fluid density vary across the mixing zone [19]. So, by attention to the importance of the mixing zone, we investigated this zone (or dispersion zone) by both of experimental and numerical models.

According to the results, the average width of the dispersion zone based on the model application and experimental results was about 2.5 cm (zone between 0.1 and 0.9 isochlors). Goswami and Clement [7] have reported the predicted dispersion zone by SEAWAT as 1 cm. Abarca and Clement [5] have used a novel approach to investigate the mixing zone in a porous media box (dimensions: 50cm × 30 cm × 2.7 cm). They have concluded that the observed mixing zone is thin near the base of the aquifer and becomes progressively thicker as the interface approaches the discharge zone. They have measured the thickness of the mixing zone at the discharge boundary (point of contact near the left chamber) as about 1.5 cm. Luyun et al. [8] have determined the mixing zone between the 0.1 and 0.9 isochlors as about 1 cm (their box dimensions were 90cm × 60cm × 8cm). Figure 6 shows the mixing zone analysis in this study.

It can be concluded that the advection is the most dominant process in our experiments. On the other hand, as the system dimensions are very small compared to the natural aquifers, so the values of dispersion and diffusion coefficients are very small and their effects may be negligible, as the photos' analysis has demonstrated this fact.

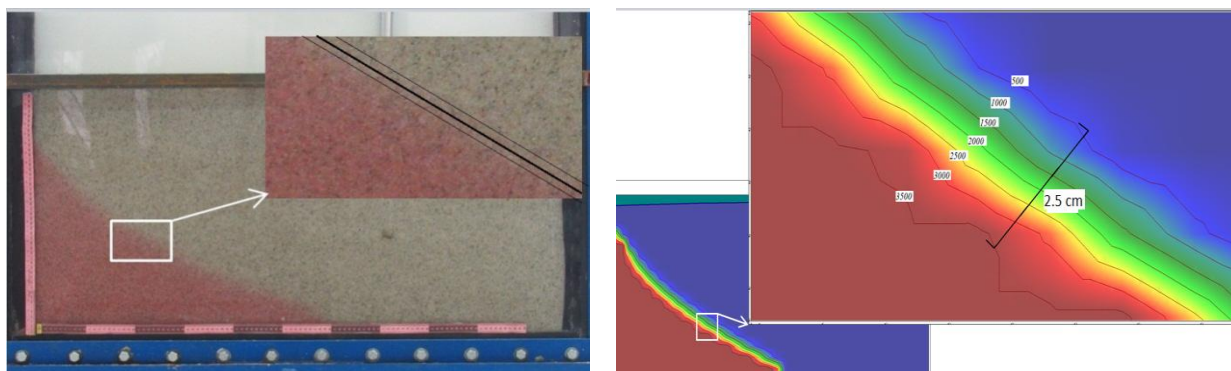


Figure 6: Dispersion effect in the mixing zone in the laboratory experiment and SEAWAT results

3.4. Velocity vectors

In this section, to further understand the SI dynamics, we analyzed the velocity vector distribution. The model predicted vector fields in above and below the saltwater wedge were used for this analysis. Figure 7 shows the wedge location along with the velocity vector directions under the first steady state condition in the experiments C1 and C2. These photos show that the freshwater almost flows in a horizontal direction and approximates the fresh-salt water interface and then turns to the direction which is parallel with the wedge. This freshwater flux floats over the saltwater in the left chamber and then flushes out through an overflow tap. Saltwater vectors show that the saltwater approximates the wedge and converges with freshwater. The conflict of these vectors creates the dispersion zone. In this mixing zone, the velocity vectors have irregular directions. This mixing state increases the dispersion effect and spreads the saltwater in the freshwater flow.

Figure 8 shows the velocity magnitude pattern in the two experiments. As shown in this figure, when the system reaches the steady state condition, saltwater flow becomes very little compared with freshwater flow. At that time, there is a little flow (or a negligible flow) from saltwater chamber and the freshwater flow reaches the wedge and overflows out through the top of saltwater chamber. As mentioned before, a small amount of saltwater flows out by spreading to the mixing zone. The pictures clearly show that the flow amounts in freshwater region and near the wedge are much more than that within the saltwater near the interface under steady state condition.

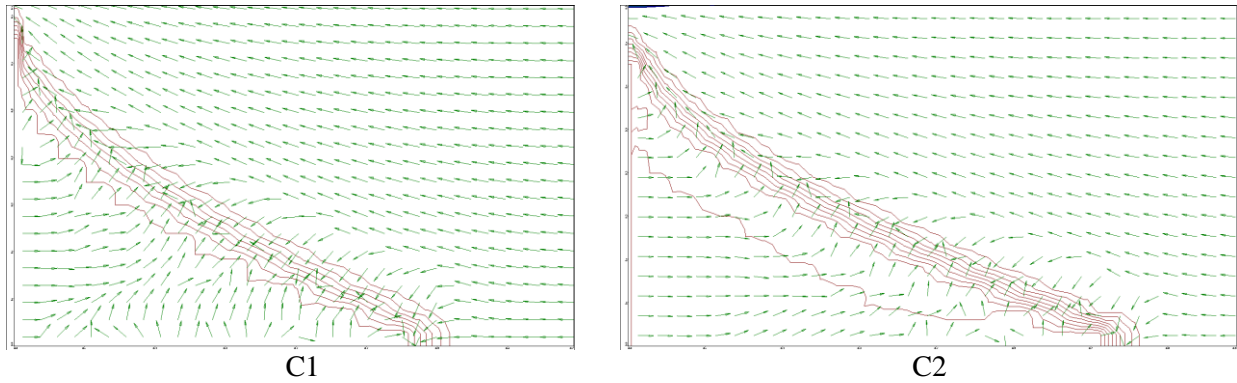


Figure 7: Velocity direction pattern of the first steady state condition in the experiments C1 and C2

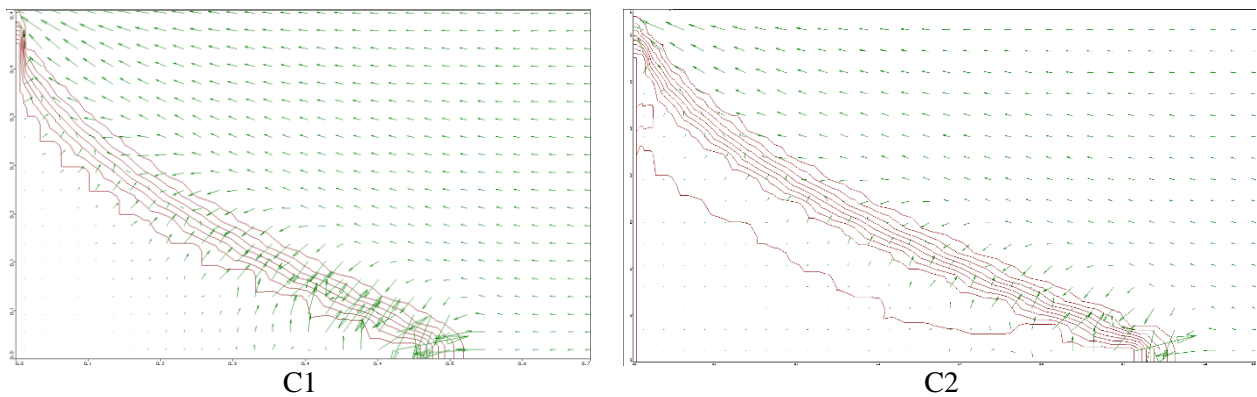


Figure 8: Velocity magnitude pattern of the first steady state condition in the experiments C1 and C2

3.5. Movement of critical points

Figure 9 shows the variation of the wedge level at the inlet and the distance of toe wedge from the coordinate origin versus the time at the intrusion stage of the test 1 in the experiments C1 and C2. The SEAWAT results are shown in this figure as lines. The results demonstrate that the model has predicted the wedge locations at its toe and also near the inlet very well.

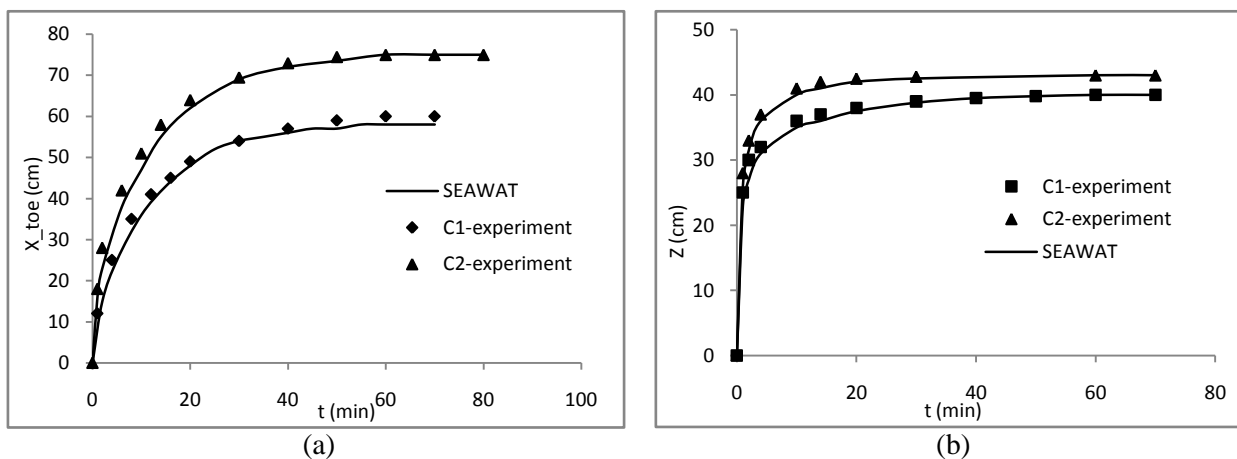


Figure 9: a) The toe position (X_{toe}) and b) the inlet wedge position (Z_w) at test 1 in the experiments C1 and C2.

As shown in the figure 9a, the tangent of intrusion rate curves at early times is high and as the time closes to the steady state condition, this rate becomes lower and lower. The wedge intrusion rates in the experiment C2 are higher than those in the experiment C1. The difference between the intrusion rates in the experiments C1 and C2 is high in early times and has a decreasing trend in time. In the experiment C2, the amount of the wedge toe

intrusion and its advance time are more than those in the experiment C1. Average intrusion rates in the experiments C1 and C2 are 1 cm/min and 1.07 cm/min respectively. According to the results, by increasing saltwater concentration the intrusion rate of the wedge and also the intrusion distance of the wedge toe into the aquifer are increased.

Figure 10 shows the toe location in the tests 2 and 3 in the both experiments C1 and C2. The markers indicate the experimental data and the lines indicate the numerical results by SEAWAT. We used this comparison to consider the interface behavior in the intrusion and recession stages. Descending parts of the charts show the recession stage of the test 2. As shown in this figure, recession rate at early times is relatively fast and it decreases as the times close to the second steady state condition. The recession rate in the experiment C2 is slightly more than that in the experiment C1. Also the wedge toe recession rate in the C2 concentration is less than that in the C1 concentration. The second and ascending part of the charts indicates the intrusion stage in the test 3. The intrusion rate in the early time of test 3 is faster than that at the test 2, also this rate in the experiment C2 is faster than similar rate in the experiment C1.

An important and interesting result in these charts is that the time of the intrusion stage is more than that of the recession stage. In other words, recession rate is faster than the intrusion rate. It implies that advancing wedge requires more time than the receding wedge to reach the steady state condition. Previously published studies also have indicated a similar trend [6, 7]. This is an important result that can play a significant role in managing and controlling the water quality of coastal aquifers [6]. The results of our experiments match with the previous studies and confirm their results.

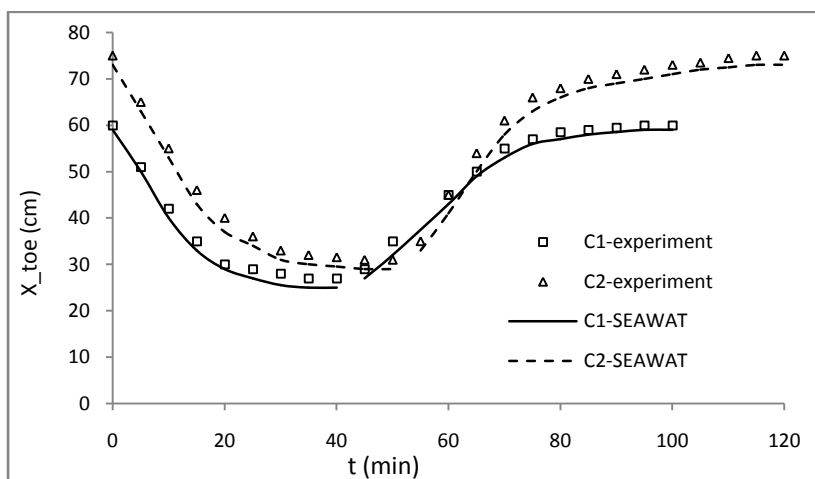


Figure 10: Comparison of toe position in intrusion and recession stages in the experiments C1 and C2

Conclusion

We studied and analyzed the saltwater intrusion into aquifer in an experimental flow tank in many aspects to better understanding the SI process in details. The most important factors in the SI processes could be the saltwater concentration and aquifer freshwater head fluctuations. For this purpose, we used two different saltwater concentrations and two different head gradient conditions. We also analyzed the intrusion and recession stages of SI and studied the differences between them. In order to further investigate the SI process and to validate our experimental results, we used a numerical method, here SEAWAT model, to simulate and analyze the detail of the obtained laboratory data. The results of the SEAWAT model in all the scenarios showed a reasonable match with the experimental data. Comparison of saltwater concentration variation results showed that the intruding wedge moved further as the concentration increased. Furthermore, the movement rates in higher concentration were faster in all times. The fresh-salt water interface was very sensitive to the head fluctuations so that changing the freshwater head by 5 cm caused the interface toe to be displaced about 30

cm. It was concluded that the interface in the intrusion stage needed more time compared with the recession stage. It means that the recession rate was faster than the intrusion rate.

Since the mixing zone between the saltwater wedge and freshwater is an important zone in groundwater issues, then we analyzed this zone through both the experimental photos and simulated conditions. Dispersion and diffusion effects caused the concentration of saltwater to vary along the mixing zone. By analyzing the obtained photos, the width of this zone was estimated as 2.5 cm. The obtained data via numerical simulations had additional and useful information about the SI which one of them was velocity vector pattern. Analyzing this pattern showed that the saltwater and freshwater converged and moved upward to the top of saltwater chamber. The conflict between the saltwater and freshwater could be a reason for creating the mixing zone. Also, analyzing the velocity vector magnitude showed that, under steady state condition, the movement of saltwater from the left chamber was very small and this small amount of the flow reached the wedge and went out along with the freshwater.

The insights gained from this study help us to better understand the saltwater intrusion processes occurring in a coastal aquifer. Also, the experimental data presented here are useful benchmarks for testing the validity of density-coupled flow and SI-predicting models. Overall the results from this study are useful for managing saltwater wedges and their better controlling.

References

1. Ketabchi H., Mahmoodzadeh M., Ataie-Ashtiani B., Simmons C. T., *Journal of Hydrology*, 535 (1) (2016) 235.
2. Chang S. W., Clement T. P., *Water Resources Research*. 48 (9) (2012) W09527.
3. Werner A. D., Bakker M., Post V. E. A., Vandenbohede A., Lu C., Ataie-Ashtiani B., Simmons C. T., Barry D. A., *Adv. Water Resour.* 51 (1) (2013) 3.
4. Bear J., Cheng A. H.-D., *Theory and Applications of Transport in Porous Media*. 14 (1999). Kluwer Academic Publishers, Dordrecht, The Netherlands.
5. Abarca E., Clement T. P., *Geophysical Research Letters*. 36 (6) (2009) L06402.
6. Chang S. W., Clement T. P., *Journal of Contaminant Hydrology*. 147 (1) (2013) 14.
7. Goswami R. R. Clement T. P., *WaterResour. Res.* 43 (4) (2007) W04418.
8. Luyun R. J., Momii K., Nakagawa K., *Journal of Hydrology*. 377 (3-4) (2009) 227.
9. Zhang Q., Volker R. E., Lockington D. A., *Journal of Contaminant Hydrology*. 49 (3-4) (2001) 201.
10. Henry H. R., Ph.D. thesis, Columbia University, New York (1960).
11. Morgan L. K., Stoeckle L., Werner A. D., Post V. E. A., *Water Resour. Res.* 49 (1) (2013) 6522.
12. Kalejaiye B. O., Cardoso S. S. S., *WaterResour. Res.* 41 (10) (2005) W10407
13. Oostrom M., Hayworth J. S., Dane J. H., Guven O., *WaterResour. Res.* 28 (8) (1992) 2123.
14. Schincariol R. A., Schwartz F. W., *WaterResour. Res.* 26 (10) (1990) 2317.
15. Simmons C. T., Pierini M. L., Hutson J. L., *Transport in Porous Media*. 47 (2) (2002) 215.
16. Johannsen K., Kinzelbach W., Oswald S., Wittum G., *Advances in Water Resources*. 25 (3) (2002) 335.
17. Zheng C., Wang P. P., U.S. Army Corps of Engineers Contract Report SERDP-99-1, (1999).

(2017) ; <http://www.jmaterenvironsci.com>